

Assembling of Dense Fluorescent Supramolecular Webs via Self-Propelled Star-Shaped Aggregates

Kirsten L. Genson,[†] Jason Holzmueller,[†] Maryna Ornatska,[†] Yong-Sik Yoo,[‡] Myoung-Hwan Par,[‡] Myongsoo Lee,[‡] and Vladimir V. Tsukruk^{*,†}

Department of Materials Science and Engineering, Iowa State University, Ames, Iowa 50010, and Department of Chemistry, Yonsei University, Seoul 120-749, Korea

Received November 21, 2005; Revised Manuscript Received January 24, 2006

ABSTRACT

We report a novel mechanism of assembly of dendronized rod molecules into a dense supramolecular fluorescent web featuring self-propelled mechanistic inward motion of star-shaped aggregates within a solution droplet. We suggest that such a motion (observed in real time) is caused by the self-repulsion of the growing star-shaped nuclei from the liquid–solid–air interface in the course of one-dimensional growth of the anchored arms. An intriguing mechanism discovered here involves microscopic (hundred micrometers) directional motion of the microscopic aggregates driven by one-dimensional molecular assembly, which opens a new venue for guided assembly of dense mesoscopic supramolecular webs. Such assemblies can serve as interesting microfluidic networks, a web of optical switches, and model systems for studying intercellular communication.

The ability to dictate the three-dimensional shape and ordering of supramolecular structures by controlling the architecture of molecular building blocks has been demonstrated on many occasions.^{1–5} Spontaneous assembly of molecules into one-dimensional structures such as ribbons, cylinders, rings, wormlike micelles, porous structures, and fibers with lengths beyond several micrometers has been shown for symmetric polyphenylene dendrimers,^{6,7} linear dendritic block copolymers,⁸ amphiphilic block-copolymers,⁹ wedge-shaped dendrons,¹⁰ amphiphilic hyperbranches,¹¹ star-shaped amphiphiles,¹² rod–coil molecules,¹³ and peptide-containing amphiphiles.¹⁴ A fine balance of π – π stacking interactions, multiple directional hydrogen bonds, entropic contributions, hydrophobic interactions, and steric constraints controlled by chemical architecture required to promote such self-assembling behavior are reasonably well established. However, the formation of dense microscopic assemblies of such one-dimensional structures is hindered by a very low threshold for interference of randomly oriented highly anisotropic one-dimensional structures. Usually, isolated domains of fibrillar agglomerates, scarcely distributed fibrils, or individual structures are reported. Moreover, the underlying kinetics and mechanism of their organization at solid substrates are rarely addressed.

In this communication, we demonstrate that a densely packed supramolecular web with fluorescent properties can be formed in the course of assembly of amphiphilic dendron–rod molecules within a solution droplet through a very peculiar mechanism of self-propelled inward motion of initial star-shaped nuclei originated at the liquid–solid–air interface (a contact line). We suggest that the type of aggregation through directional self-propelled motion is caused by the mechanistic motion of star-shaped aggregates via repulsion of pinned arms during their one-dimensional growth.

Rod–dendron molecules composed of three hydroxyl-terminated tetra-branched ethylene oxide chains attached to a rigid octa-*p*-phenylene stem at the first and second phenyl rings were synthesized by the method reported previously (Figure 1).¹⁵ Dendrons were dissolved in 1-octanol (0.5 mM and 5 mM concentrations) and adsorbed onto glass, quartz, silicon, and HOPG substrates. The solvent was allowed to evaporate slowly (24 h) at room temperature at the microscopic stage, and elapsed video has been used to record the kinetics of assembly. The compound could not be dissolved in ethylene glycol and ethanol and did not form any fibrillar structures after casting from phenyloctane and chloroform. We believe that there are several factors that work in favor of octanol: the compound is well soluble in this solvent, the solvent does not interfere with staking of phenylene-rich segments, and the solvent wets the graphite surface nicely. Moreover, very slow (several hours) evaporation

*To whom correspondence should be addressed. E-mail: Vladimir@iastate.edu.

[†] Iowa State University.

[‡] Yonsei University.

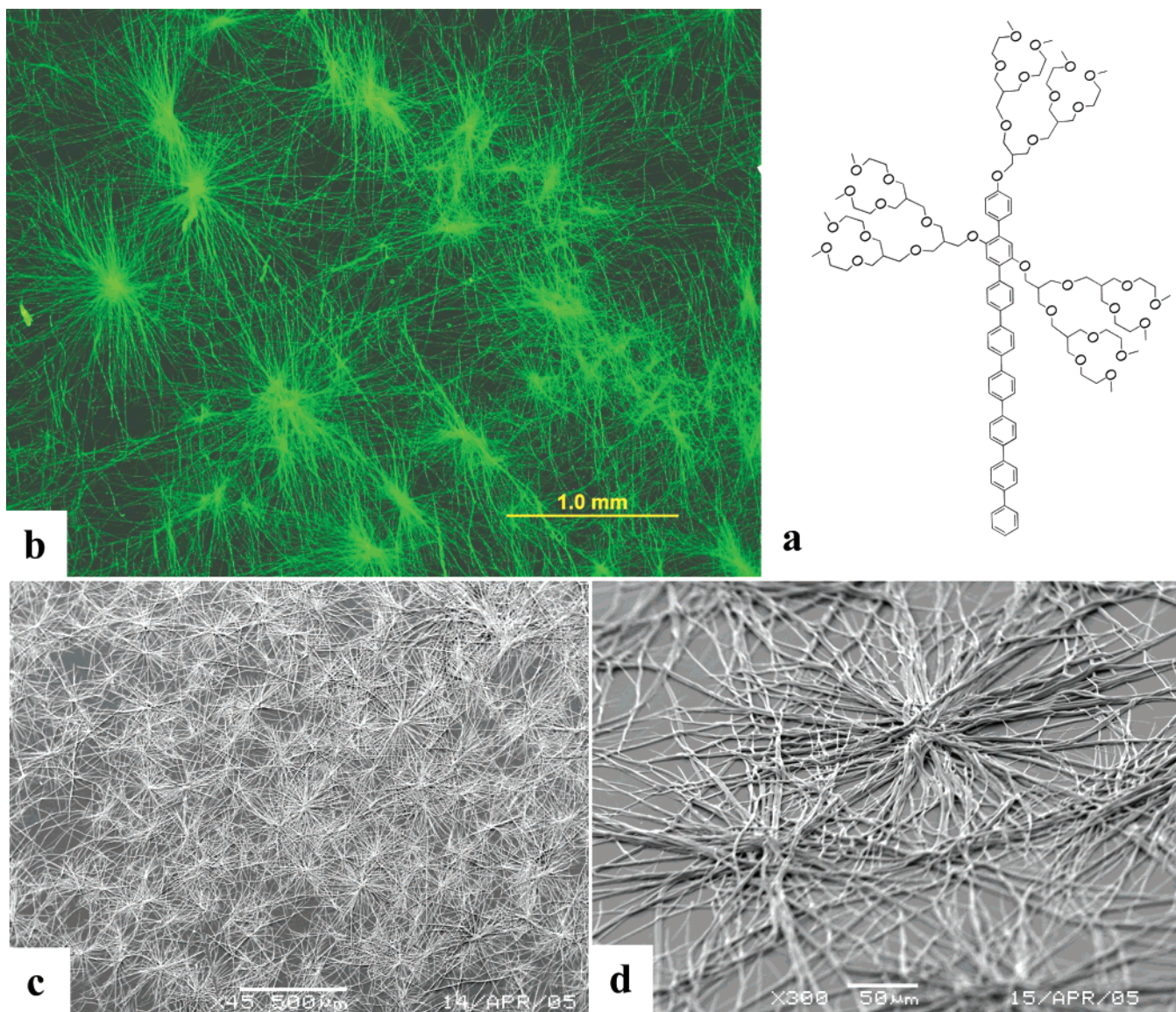


Figure 1. (a) Chemical formula of treelike rod–dendrons; (b) Fluorescent micrograph of a dense network of one-dimensional structures; (c) SEM image of dense network of star-shaped aggregates at graphite surface; (d) closer look at star-shaped aggregates (SEM image at an angle).

provides a steady increase of the concentration along the contact line and the best conditions for crystallization of solute.

Spontaneous self-assembly of these amphiphilic dendron–rod molecules with steric mismatch of bulkier dendronized polar heads and rigid stems into one-dimensional structures was observed at the air–solvent interface within a droplet of concentrated solution spread on hydrophobic HOPG graphite (Figure 1). The dense web formed by star-shaped aggregates possesses intense fluorescence caused by the energy transfer between herringbone packed rigid rods assembled into nanoscale clusters as has been discussed earlier.¹⁵ Casting on other substrates resulted in a much less dense and developed network. Octanol, a nonvolatile solvent, provided for the long lifetime of the droplet (24 h), uniform dispersion, and perfect wetting, thus allowing for the uniform casting and the formation of a dense fluorescent web. The star-shaped aggregates are composed of well-defined and

uniform cores about 50 μm across with multiple bundled arms extending from the cores and interacting with other aggregates separated by 200–1000 μm depending upon the solution concentration (Figure 1c and d). Most of the straight arms are extended over several hundred micrometers with some of them exceeding several millimeters, an unprecedented continuity for organic supramolecular structures. The formation of such continuous one-dimensional aggregates is very different from spherical and circular aggregation observed in THF and at the air–water interface^{15,16} and can be associated with continuous growth of dendronized rods in a solvent selective for PEO branches and readily wetting a graphite substrate.

An SEM image of the web on a solid substrate showed a single layer (conditions were selected to avoid any significant material built-up) of elevated cores composed of tightly packed bundles of fibrils with multiple straight arms extending from the cores and intersecting other arms from

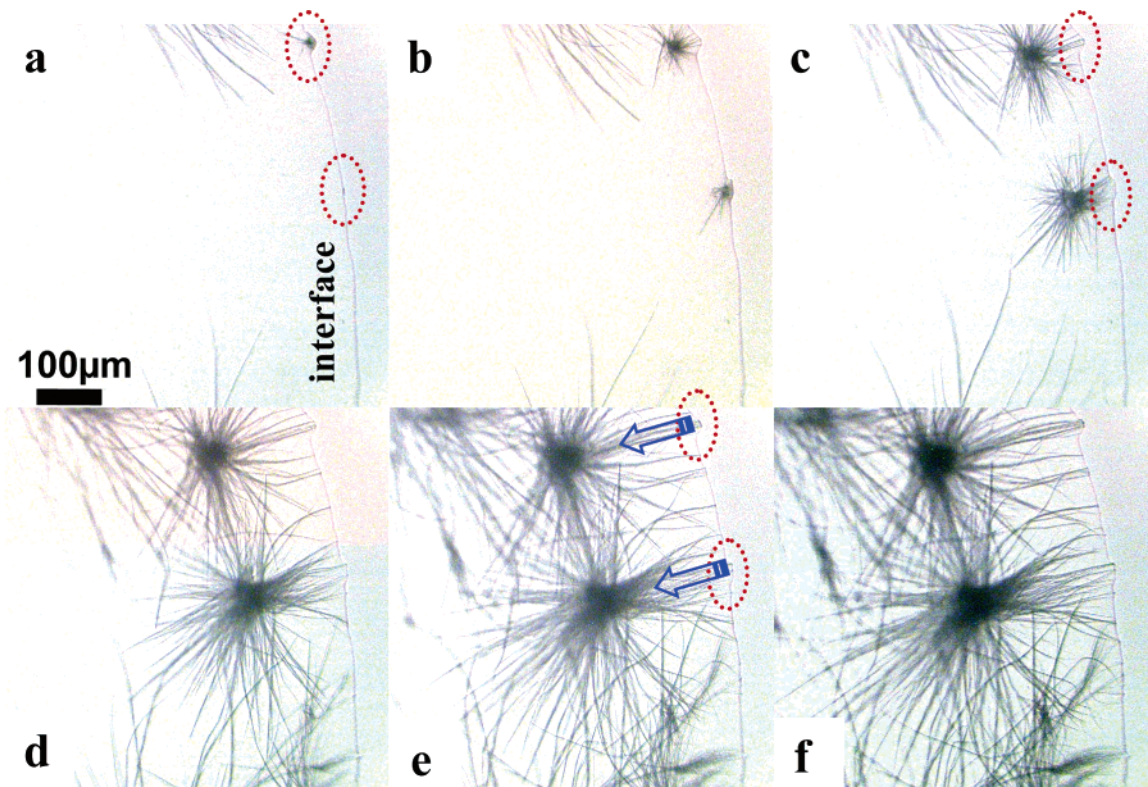


Figure 2. Time-lapse optical micrographs of growth video after (a) 40, (b) 50, (c) 60, (d) 100, (e) 140, and (f) 180 min from solution deposition on a graphite surface (for elapsed video see the Supporting Information). Marks indicate original locations of nuclei and their movement from the interface toward the droplet center.

neighboring aggregates (Figure 1). These arms are very flexible as indicated by their easy deformation at intersection points allowing them to run above or below another arm (not shown). The formation of such a dense planar web is unusual for highly anisotropic one-dimensional aggregates, and the overall web morphology closely resembled a neuron network grown on a planar substrate.¹⁷

The cause for the dense web formation was revealed in the course of direct in situ monitoring of its growth with optical microscopy (Figure 2). Initial stages of the web growth displayed the nucleation of bundle clusters at the selected locations with higher curvature along the contact line (Figure 2a). Optical micrographs revealed the number of bundles radiating from clusters, which were multiplied and rapidly extended in all directions giving rise to the star shape of these aggregates. After the initial formation of the star-shaped nuclei (within 2 h), the faster growth of the star-shaped aggregates was observed with thickening—lengthening of the bundles creating straight arms with very high aspect ratios reaching 500–1000.

But the most astonishing observation is the rapid mechanistic motion of the forming star aggregates outward from the original points of nucleation and inward of the droplet as can be seen in Figure 2b–e and in the real-time-lapse video in the Supporting Information. The star aggregates are moving in an inward direction toward the center of the droplet and far from the interface. We suggest that the self-propelled motion is driven by the repulsive forces between the pinned growing bundles and the contact line. The one end of growing bundles is arrested by the interface, thus

effectively creating a single-point confinement. Corresponding forces along the lengthening arms act on the core, which is freely suspended in the solution, thus creating compressive stress in the radial direction. This stress is effectively applied to the mobile core, which is moved out of the original location at the interface to free more space for the lengthening bundles. However, the entropy should also contribute considering that the placement of highly branched star-shaped aggregates in the vicinity of the contact line results in some unfavorable entropy loss.

This motion creates a dense network of cores “gathered” together near the center and removed from the interface. The trajectory of core motion marked in Figure 2 is virtually perpendicular to the contact line, and the growing bundles are also oriented perpendicular to the interface. At the final stage, the star-shaped aggregates began interacting with each other, slowing the motion and bending some arms to accommodate their dense arrangement. The final length (200–3000 micrometers) of the one-dimensional structures was 2–3 orders of magnitude higher than the average bundle diameter (3.0 ± 2.0 micrometers).

The assembly observed here suggests that the directional microscopic motion is caused by the aggregate self-propelling. The feasibility of this suggestion can be supported by estimations of corresponding diffusion and energetic terms. First, the Avrami analysis of the growth kinetics¹⁸ confirmed the one-dimensional mode of bundle growth visible in optical images with the effective rate of 40–150 nm/sec. Second, the rate of one-dimensional growth, average bundle cross section, and molecular dimensions (effective length of 5 nm

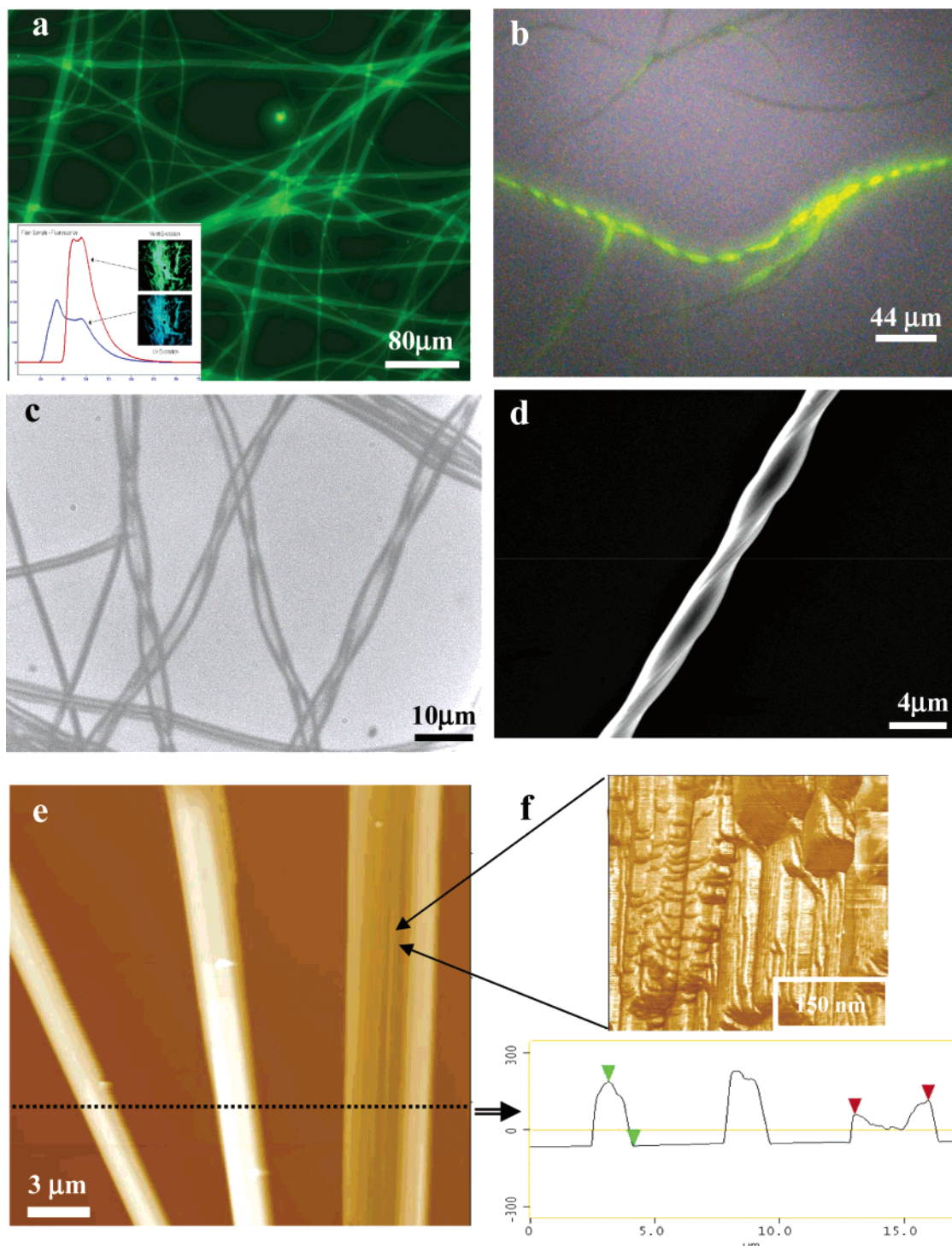


Figure 3. (a) Higher magnification fluorescent micrograph of network; the inset shows fluorescence spectra under two different excitations. (b) Fluorescent micrograph of a twisted arm of the star-shaped aggregate. (c) Optical micrograph of twisted tubular arms. (d) Higher resolution SEM image of a twisted arm. (e) AFM topography image of fibrillar and collapsed tubular arms, z range 300 nm. (f) Cross section of different arms along with a high-resolution AFM image of the top area.

and diameter of 2 nm) allow for the estimation of the diffusion coefficient (D) to be equal to $1.5\text{--}4.5 \times 10^{-8} \text{ cm}^2/\text{s}$. This value is within the range of values $0.8\text{--}4 \times 10^{-8} \text{ cm}^2/\text{s}$ measured for diffusion of ethylene oxide chains with different lengths¹⁹ (dendritic component of molecules), thus confirming that the observed rate of bundle growth is compatible with the diffusion rate of dendritic molecules to the growing facet.

Finally, the forces that should be exerted to sustain the mechanistic motion of the aggregate can be estimated assuming that a fraction of bundles (10–20) should propel the star aggregate with the estimated mass of 100 ng within a solution with viscosity 0.1 P. This estimation gives very negligible viscous contribution (as evaluated from the Stokes equation) and the total forces of about 10 nN per arm assuming the worst case scenario of lifting against gravita-

tional forces. Considering that a number of molecules required to diffuse to a bundle cross-section (1–3 micrometers) is within 10^4 – 10^5 , we can estimate the force required to be generated by a single assembling molecule to be within 0.1–2 pN. This value is well below the rupturing forces for organic molecules (1–5 nN) and is close to typical forces exerted by elastically deformed polymer chains.²⁰ Thus, the local stresses generated by propelling the large aggregate through the solution can be sustained by organic molecules and can be overcome by collectively interacting assembled molecules. In addition, from the very slow rate of evaporation we estimated that possible inward flow of solution would be extremely slow, well below the aggregate velocity observed here.

Further scrutiny of the fibrillar bundles reveals various inner structures depending upon their dimensions and stages of growth. We will describe them here briefly, and a detailed discussion will be published in a forthcoming paper. High-resolution optical microscopy from bundles with a diameter of 3–15 μm showed transparent cores coupled with the opaque edge, suggesting a tubular structure of the one-dimensional structures in solution (Figure 3). Strong fluorescence was observed for this fibrillar network with two fluorescence peaks dependent on exciting radiation. Fluorescence bands at 437 and 470 nm were observed for the ribbon structures illuminated with a 365-nm ultraviolet wavelength (Figure 3a inset). Illuminated with 405-nm wavelength, the fibrils were observed to fluoresce at 470 and 489 nm. The multiple fluorescence peaks yielded from two dissimilar π – π stacking conformations suggests a more specific crystalline structure of the self-assembled ribbons.²¹ The treelike rod–dendrons formed a herringbone structure in bulk, thus forming two π – π stacking conformations similar to the structure for the 1D ribbon formation presented below. The red shift of the peaks and reduced intensity observed for the shorter wavelength suggests quenching of the fluorescent behavior due to the close-packed ordering of the rigid phenylene rods.

After drying, collapsed tubular structures with elevated edges and a lower central region were observed for these bundles in AFM images (Figure 3e). Smaller one-dimensional structures with diameters of 1–3 μm showed uniform fluorescence indicating uniform fibrillar structures and, finally, a ribbonlike shape was observed for structures with the smallest dimensions (below 300 nm). High-resolution AFM shows a lamellar structure of the fibril top areas consistent with X-ray data (Figure 3f). Indeed, X-ray diffraction shows high crystallinity of these structures combined with a primitive orthorhombic lattice assembled into nanoscale clusters similar to those suggested for the bulk material (Figure 4).¹⁵ The calculated unit cell of $a = 2.4$ nm, $b = 1.9$ nm, and $c = 4.8$ nm for the crystal structure of the ribbons is very close to the bulk supercell structure reported previously.¹⁵ The treelike molecules formed a supercell structure with the rod cores oriented horizontally along the a direction (Figure 4). The one-dimensional self-assembled structure had high degree of crystallinity, comparable to the bulk material, suggesting an analogous

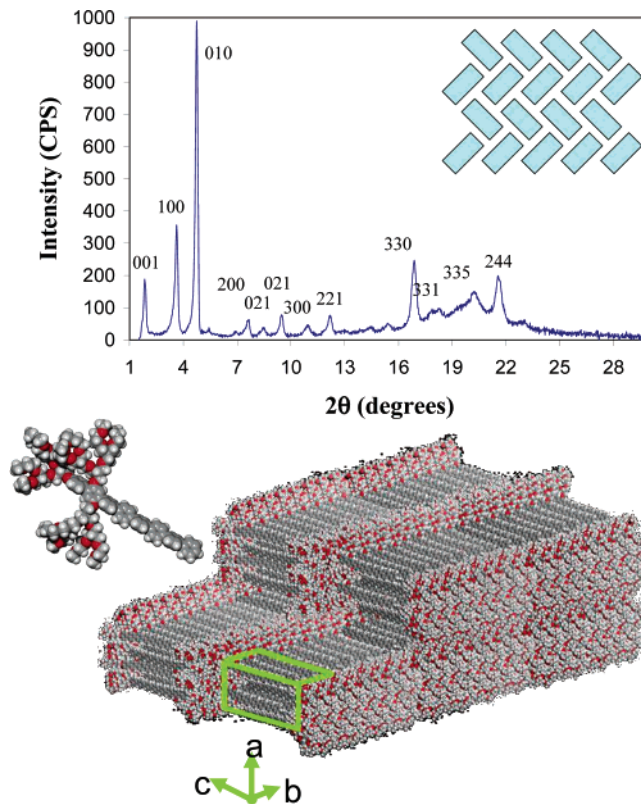


Figure 4. X-ray diffraction of the resulting web with peaks labeled for the unit cell with herringbone packing (inset, top); molecular model of 1D ribbon structure with the unit cell orientation and a single molecule.

herringbone alignment of the rod–dendron molecules. The herringbone ordering of the molecules allows for π – π interactions between parallel rods as well as between rods that are angled.

The striking feature discovered for these one-dimensional aggregates was the observation of twisted structures with a pitch of several micrometers observed on both optical and fluorescent microscopy images (Figure 3b and c). Twisting of the tubular structures was also confirmed with high-resolution SEM, clearly showing ridges of the twisted morphology (Figure 3d). The pitch was extremely large and only a fraction of the fibrillar structures display twisted morphology with the majority of them possessing uniform shape. Interestingly, the twisted microfibrils usually exhibit much greater fluorescence in comparison with the straight structures. We can speculate that this intriguing phenomenon could be related to breaking the packing symmetry in deformed one-dimensional assemblies, which inhibit fluorescence quenching.

As known, helical morphology is observed frequently for one-dimensional structures composed of molecules with asymmetrical shapes and chiral centers. Their helical pitch is usually comparable to molecular dimensions and is caused by steric constraints for molecular packing.²² Considering the features of the twisted structures observed here and the mechanism of growth through self-propelled motion, we suggest that the twisting of these structures occurs because of stresses developed in arms interacting with interface or

neighboring aggregates. Such twisting can occur if compression is slightly nonaxial, stress is directed at an angle, and a deformation releases the stresses associated with the transversal component of the biaxial compression.²³

In conclusion, we observed a novel mechanism of self-assembly of a dense web of star-shaped aggregates due to their self-propelled mechanistic motion. Such a correlated motion toward the center of the droplet is caused by the self-repulsion of the nuclei from the liquid–solid–air interface in the course of molecular assembly of dendritic molecules, resulting in one-dimensional growth of pinned arms. Such a mechanism that involves microscopic (hundred micrometers) directional motion of whole aggregates driven by one-dimensional molecular assembly has never been reported before and opens new venues for guided assembly of star-shaped molecular aggregates composed of multiple microscopic tubules into dense mesoscopic webs. This web can be dissolved easily in the solvent used for casting but remains stable under a variety of other solvents as well as at modestly elevated temperatures. For future developments we could envision controlling the nucleation process by making organized patterns of critical nuclei by, for example, micro-patterning the solid support, thus assembling regular dense webs. Such organized networks can serve as interesting models for microfluidic networks, webs of optical switches, dense webs for entrapping cells, and model systems for studying intercellular communication.²⁴

Acknowledgment. We thank S. Ricchio and D. McNeal at Leeds Precision Instruments for fluorescence micrographs and Jim Thorne at Craic Technologies for fluorescence spectra. Support from the Institute for Soldier Nanotechnologies, MIT for V.V.T.'s visit and SEM study, and funding from the U.S. National Science Foundation (DMR-038982), AFOSR (FA9550-05-1-0209) and Creative Research Initiative Program of the Korean Ministry of Science and Technology are gratefully acknowledged.

Supporting Information Available: Time-lapse video of growth. This material is available free of charge via the Internet at <http://pubs.acs.org>.

References

- (1) (a) Stupp, S. I.; LeBonheur, V.; Walker, K.; Li, L. S.; Huggins, K. E.; Keser, M.; Amstutz, A. *Science* **1997**, *276*, 384. (b) Hartgerink, J. D.; Beniash, E.; Stupp, S. I. *Science* **2001**, *294*, 1684.
- (2) (a) Percec, V.; Glodde, M.; Bera, T. K.; Miura, Y.; Shiyonovskaya, I.; Singer, K. D.; Balagurusamy, V. S. K.; Heiney, P. A.; Schnell, I.; Rapp, A.; Spiess, H.-W.; Hudson, S. D.; Duank, H. *Nature* **2002**, *419*, 384. (b) Zeng, X.; Ungar, G.; Liu, Y.; Percec, V.; Dulcey, A. E.; Hobbs, J. K. *Nature* **2004**, *428*, 157. (c) Percec, V.; Dulcey, A. E.; Balagurusamy, V. S. K.; Miura, Y.; Smidrkal, J.; Peterca, M.; Nummelin, S.; Edlund, U.; Hudson, S. D.; Heiney, P. A.; Duan, H.; Maganov, S. N.; Vinogradov, S. A. *Nature* **2004**, *430*, 764. (d) Gopalan, P.; Li, X.; Li, M.; Ober, C. K.; Gonzales, C. P.; Hawker, C. J. *J. Polym. Sci.* **2003**, *41*, 3640.
- (3) Lee, M.; Cho, B.-K.; Zin, W.-C. *Chem. Rev.* **2001**, *101*, 3869.
- (4) (a) Loi, S.; Butt, H.-J.; Hampel, C.; Bauer, R.; Wiesler, U.-M.; Mullen, K. *Langmuir* **2002**, *18*, 2398. (b) Loi, S.; Wiesler, U.-W.; Butt, H.-J.; Mullen, K. *Macromolecules* **2001**, *34*, 3661. (c) Jang, W.-D.; Aida, T. *Macromolecules* **2004**, *37*, 7325.
- (5) Tsukruk, V. V. *Prog. Polym. Sci.* **1997**, *22*, 247.
- (6) Loi, S.; Wiesler, U.-M.; Butt, H.-J.; Mullen, K. *Chem. Commun.* **2000**, 1169.
- (7) (a) Liu, D.; De Feyter, S.; Grim, P. C. M.; Vosch, T.; Grebel-Koehler, D.; Wiesler, U.-M.; Berresheim, A. J.; Mullen, K.; De Schryver, F. C. *Langmuir* **2002**, *18*, 8223. (b) Liu, D.; Feyter, S. D.; Cotlet, M.; Wiesler, U.-M.; Weil, T.; Herrmann, A.; Mullen, K.; De Schryver, F. C. *Macromolecules* **2003**, *36*, 8489.
- (8) Cho, B.-K.; Jain, A.; Gruner, S. M.; Wiesner, U. *Science* **2004**, *305*, 1598.
- (9) (a) Jain, S.; Bates, F. S. *Science* **2003**, *300*, 460. (b) Discher, D. E.; Eisenberg, A. *Science* **2002**, *297*, 967. (c) Pochan, D. J.; Chen, Z.; Cui, H.; Hales, K.; Qi, K.; Wooley, K. L. *Science* **2004**, *306*, 94.
- (10) Ungar, G.; Liu, Y.; Zeng, X.; Percec, V.; Cho, W.-D. *Science* **2003**, *299*, 1208.
- (11) (a) Ornatska, M.; Peleshanko, S.; Rybak, B.; Holzmüller, J.; Tsukruk, V. V. *Adv. Mater.* **2004**, *16*, 2206. (b) Ornatska, M.; Bergman, K.; Rybak, B.; Peleshanko, S.; Tsukruk, V. V. *Angew. Chem.* **2004**, *43*, 5246. (c) Ornatska, M.; Peleshanko, S.; Genson, K. L.; Rybak, B.; Bergman, K. N.; Tsukruk, V. V. *J. Am. Chem. Soc.* **2004**, *126*, 9675.
- (12) Genson, K. L.; Hoffman, J.; Teng, J.; Zubarev, E. R.; Vaknin, D.; Tsukruk, V. V. *Langmuir* **2004**, *20*, 9044.
- (13) (a) Tsukruk, V. V.; Genson, K. L.; Peleshanko, S.; Markutsya, S.; Greco, A.; Lee, M.; Yoo, Y. *Langmuir* **2003**, *19*, 495. (b) Leclere, Ph.; Hennebicq, E.; Calderone, A.; Brocorens, P.; Grimsdale, A. C.; Mullen, K.; Bredas, J. L.; Lazzaroni, R. *Prog. Polym. Sci.* **2003**, *28*, 55. (c) Leclere, Ph.; Surin, M.; Jonkheijm, P.; Henze, O.; Schenning, A. P. H. J.; Biscarini, F.; Grimsdale, A. C.; Feast, W. J.; Meijer, E. W.; Mullen, K.; Bredas, J. L.; Lazzaroni, R. *Eur. Polym. J.* **2004**, *40*, 885.
- (14) Messmore, B. W.; Hulvat, J. F.; Sone, E. D.; Stupp, S. I. *J. Am. Chem. Soc.* **2004**, *126*, 14452.
- (15) Yoo, Y.-S.; Choi, J.-H.; Song, J.-H.; Oh, N.-K.; Zin, W.-C.; Park, S.; Chang, T.; Lee, M. *J. Am. Chem. Soc.* **2004**, *126*, 6294.
- (16) Holzmüller, J.; Genson, K. L.; Park, Y.; Yoo, Y.-S.; Park, M.-H.; Lee, M.; Tsukruk, V. V. *Langmuir* **2005**, *21*, 6392.
- (17) Levitan, I. B.; Kaczmarek, L. K. *The Neuron: Cell and Molecular Biology*; Oxford University Press: New York, 1991.
- (18) Avrami, M. J. *Chem. Phys.* **1940**, *8*, 212.
- (19) Georges, J. *Spectrochim. Acta, Part A* **2003**, *59*, 519.
- (20) (a) Zou, S.; Schonherr, H.; Vancso, G. J. *Angew. Chem., Int. Ed.* **2005**, *44*, 956. (b) Merkel, R.; Nassoy, P.; Leung, A.; Ritchies, K.; Evans, E. *Nature* **1999**, *397*, 50. (c) Evans, E. *Annu. Rev. Biophys. Biomol. Struct.* **2001**, *30*, 105.
- (21) Helfer, C. A.; Mendicuti, F.; Mattice, W. L. In *Comprehensive Desk Reference of Polymer Characterization and Analysis*; Brady, R. F., Jr., Ed.; Oxford University Press: New York, 2003.
- (22) (a) Hill, J. P.; Jin, W.; Kosaka, A.; Fukushima, T.; Ichihara, H.; Shimomura, T.; Ito, K.; Hashizume, T.; Ishii, N.; Aida, T. *Science* **2004**, *304*, 1481. (b) Cornelissen, J. J. L. M.; Fischer, M.; Sommerdijk, N. A. J. M.; Nolte, R. J. M. *Science* **1998**, *280*, 1427. (c) Leclere, P.; Surin, M.; Lazzaroni, R.; Kilbinger, A. F. M.; Henze, O.; Jonkheijm, P.; Biscarini, F.; Cavallini, M.; Feast, W. J.; Meijer, E. W.; Schenning, A. P. H. J. *J. Mater. Chem.* **2004**, *14*, 1959.
- (23) Audoly, B.; Roman, B.; Pocheau, A. *Eur. Phys. J. B* **2002**, *27*, 7.
- (24) Silva, G. A.; Czeisler, C.; Niece, K. L.; Beniash, E.; Harrington, D. A.; Kessler, J. A.; Stupp, S. I. *Science* **2004**, *303*, 1352.

NL052301I